

Fine structure of an exciton coupled to a single Fe^{2+} ion in a CdSe/ZnSe quantum dot

T. Smoleński,* T. Kazimierczuk, M. Goryca, W. Pacuski, and P. Kossacki

Institute of Experimental Physics, Faculty of Physics, University of Warsaw, ul. Pasteura 5, 02-093 Warsaw, Poland

(Received 21 February 2017; published 5 October 2017)

We present a polarization-resolved photoluminescence study of the exchange interaction effects in a prototype system consisting of an individual Fe^{2+} ion and a single neutral exciton confined in a CdSe/ZnSe quantum dot. A maximal possible number of eight fully linearly polarized lines in the bright exciton emission spectrum is observed, evidencing complete degeneracy lifting in the investigated system. We discuss the conditions required for such a scenario to take place: anisotropy of the electron-hole interaction and the zero-field splitting of the Fe^{2+} ion spin states. Neglecting either of these components is shown to restore partial degeneracy of the transitions, making the excitonic spectrum similar to those previously reported for all other systems of quantum dots with single magnetic dopants.

DOI: [10.1103/PhysRevB.96.155411](https://doi.org/10.1103/PhysRevB.96.155411)

I. INTRODUCTION

A single quantum dot (QD) containing an individual transition metal ion provides an excellent opportunity to study the spin properties of a localized magnetic impurity interacting with the semiconductor lattice and confined band carriers in isolation from any other ions in the sample [1]. The variety of magnetic dopants with a partially filled $3d$ shell that can be incorporated into QDs of different III-V or II-VI materials offers a wide range of combinations, which can be chosen in order to achieve the desired properties of a magnetic-ion-QD system, e.g., long spin-relaxation time [2–5]. This idea has been brought to life by the discovery of the fact that a single ion embedded inside the QD does not introduce any nonradiative excitonic recombination channels even for wide-energy-gap QDs [2,3]. This finding has extended the optical studies of QDs doped with individual ions from the two classical systems of CdTe/ZnTe [1,6–15] and InAs/GaAs [16–18] QDs with single Mn^{2+} ions to novel systems such as CdSe/ZnSe QDs with single Mn^{2+} [2,3,19] and Fe^{2+} [20] ions or CdTe/ZnTe QDs with single Co^{2+} [2,21] and Cr^{2+} [22–24] ions. For all of these systems, despite the different electronic configurations of the magnetic ions, the ion ground energy level was found to be an orbital singlet exhibiting an effective spin S . The degeneracy of the $2S + 1$ ion spin states is lifted by the interaction with the strained semiconductor lattice as well as the spin-orbit coupling. In the leading order, the resulting magnetic anisotropy can be described by the term DS_z^2 , where z corresponds to the QD growth axis. The value of the parameter D is relatively small ($\sim \mu\text{eV}$) for an isoelectronic Mn^{2+} ion [11–14] and a few orders of magnitude larger for ions with a nonzero orbital momentum [2,20–22,25]. As such, in the case of ions like Fe^{2+} or Cr^{2+} , only the subspace of some lowest-energy $|S_z\rangle$ ion states is available at low temperatures.

The optical access to the subspace of thermally populated ion spin states is granted by the $s,p-d$ exchange interaction between the ion and a neutral exciton (X) confined inside the QD [26]. Such an interaction splits the excitonic energy levels, which gives rise to the presence of a multitude of lines in the X photoluminescence (PL) spectrum [1,2,16,20,22]. The general

character of this spectrum is, however, qualitatively different for a QD containing an ion with half-integer and integer spin S . In the former case, the Kramers rule protects the twofold degeneracy of the energy levels for both initial and final states of the excitonic recombination. As a consequence, the resulting X optical transitions are at least doubly degenerate, which does not allow us to address the half-integer-spin states of the ion based solely on the energies of the X PL lines. Instead, the unequivocal readout of the half-integer spin of the magnetic dopant requires us to monitor both the energies and polarizations of the emitted photons, as experimentally demonstrated for the Mn^{2+} and Co^{2+} ions in II-VI QD systems [1,2]. A fundamentally different physical picture holds for the magnetic ion with an integer spin, which does not warrant Kramers degeneracy. In this case, all of the X optical transitions may have different energies. This implies that, in principle, the PL spectrum of an optically active bright exciton X_b of two possible spin configurations may consist of $2N^2$ distinct emission lines, where N is the number of thermally populated integer-spin states of the magnetic ion. However, reaching this theoretical limit requires both the ion and the exciton spin states to be substantially mixed, which would allow the optical transitions between each initial and each final state of the X recombination. Up to now, such conditions have not been met for any QD systems doped with single integer-spin ions, as the number of experimentally observed excitonic emission lines in all of the previous studies [1–24,27] was always well below $2N^2$.

Here we provide direct experimental proof showing that the bright exciton PL spectrum from a QD with an integer-spin magnetic ion may feature all possible $2N^2$ optical transitions of different energies. This finding is revealed by our polarization-resolved PL studies of CdSe/ZnSe QDs doped with single Fe^{2+} ions ($S = 2$). Owing to large Fe^{2+} magnetic anisotropy [20], this system is characterized by a relatively small subspace of the $N = 2$ lowest-energy ion spin states with $S_z = \pm 2$ that are available at low temperatures. We present experimental data showing that, in general, the X PL spectrum in such a QD indeed consists of eight distinct emission lines, each of them being fully (linearly) polarized as expected for nondegenerate transitions. Such a character of the excitonic spectrum is demonstrated to be due to the interplay of three different interactions: the $s,p-d$ exchange coupling between the ion and

*Tomasz.Smolenski@fuw.edu.pl

X, the anisotropic electron-hole exchange mixing the two spin states of the bright exciton, and the spin-orbit coupling mixing the two $S_z = \pm 2$ spin states of the Fe^{2+} ion. We show that a simple spin Hamiltonian model including these interactions fully reproduces the energies, relative oscillator strengths, and polarization properties of the X emission lines. Additionally, we demonstrate that this model extended with the exciton and ion Zeeman terms provides also a correct description of the excitonic PL spectrum evolution in the magnetic field applied in the Faraday geometry.

II. SAMPLES AND EXPERIMENTS

Our experiments were performed on a sample grown by molecular beam epitaxy (MBE). It consisted of a single layer of self-organized CdSe:Fe QDs embedded in a ZnSe barrier [20]. The concentration of iron doping was adjusted to maximize the probability of finding a QD containing exactly one Fe^{2+} ion. For the optical experiments, the sample was immersed in pumped liquid helium ($T = 1.8$ K) inside a magneto-optical cryostat equipped with a superconducting magnet producing a magnetic field of up to 10 T in the Faraday geometry. The PL was excited using a continuous-wave Ar-ion laser at 488 nm. A reflective-type microscope objective (numerical aperture of 0.72) attached directly to the sample surface was used to focus the laser to a submicrometer spot and to collect the PL signal from the QDs. The collected PL was then resolved using either a 0.5- or 0.75-m monochromator and recorded with a CCD camera. A set of polarization optics placed in the signal beam (including a linear polarizer, $\lambda/2$ - and $\lambda/4$ -wave plates) enabled us to perform the PL measurements with either linear or circular polarization resolution.

III. EXPERIMENTAL RESULTS

Our studies of the fine structure of the excitonic emission in a QD with a single Fe^{2+} ion were performed on a number of randomly selected dots. The representative examples of the X PL spectra obtained for the two different Fe-doped QDs are presented in Figs. 1(a) and 1(b). In the case of QD1 [Fig. 1(a)], the spectrum features a familiar two-line fine structure, which was previously established in Ref. [20]. The splitting between these lines arises mainly from the $s, p-d$ exchange interaction between the exciton and the resident ion. Due to the large magnetic anisotropy of the Fe^{2+} ion as well as the heavy-hole character of the excitonic ground state in the QD, this exchange interaction is effectively Ising-like and takes the general form of $J_z S_z$, where J_z and S_z are the z components of the excitonic and Fe^{2+} spin operators (with z being the quantization axis of both the hole and the Fe^{2+} ion spins, i.e., the QD growth axis). As a result, the $s, p-d$ exchange splits four spin configurations $|J_z, S_z\rangle$ of the bright-exciton- Fe^{2+} system into two subspaces consisting of states corresponding to antiparallel and parallel spin orientations of X_b and the Fe^{2+} ion, i.e., $|\mp 1, \pm 2\rangle$ and $|\pm 1, \pm 2\rangle$, respectively. These two groups of states are separated by the energy of Δ_{sp-d} (see Fig. 2), which results in the presence of two distinct lines in the X PL spectrum. Such a character of the X emission remains unaltered also after taking into account the anisotropic part of the electron-hole exchange interaction δ_1 [28–30], which is

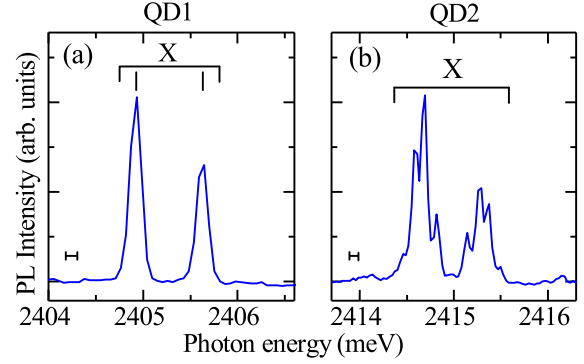


FIG. 1. PL spectra of the neutral exciton in two different CdSe/ZnSe QDs containing single Fe^{2+} ions. The spectra were measured without polarization resolution. (a) QD1 with negligible δ_{Fe} splitting of the two Fe^{2+} ground states. (b) QD2 exhibiting large δ_{Fe} splitting as well as a strong anisotropic part of the electron-hole exchange interaction. Note that the spectral resolution of the QD1 spectrum is approximately 1.5 times lower than in the case of QD2, which is due to the shorter length of the monochromator used. The approximate values of both resolutions are schematically marked by horizontal bars displayed on the left side of each spectrum.

relatively strong in the case of the studied CdSe/ZnSe QDs [31–34]. The electron-hole exchange couples the two spin states $J_z = \pm 1$ of the bright exciton associated with the same Fe^{2+} ion spin projection S_z . Consequently, it increases the splitting between the two subspaces of the X_b - Fe^{2+} states to $\sqrt{\Delta_{sp-d}^2 + \delta_1^2}$ (as depicted in Fig. 2) but does not lift the twofold degeneracy of these subspaces, thus preserving the two-line pattern of the excitonic emission.

The physical picture turns out to be qualitatively different if, apart from the $s, p-d$ and electron-hole exchange interactions, a third interaction, which mixes the two Fe^{2+} ion spin states $S_z = \pm 2$, also exists. Such a mixing is characteristic of the magnetic ion with an integer spin, and for the Fe^{2+} ion

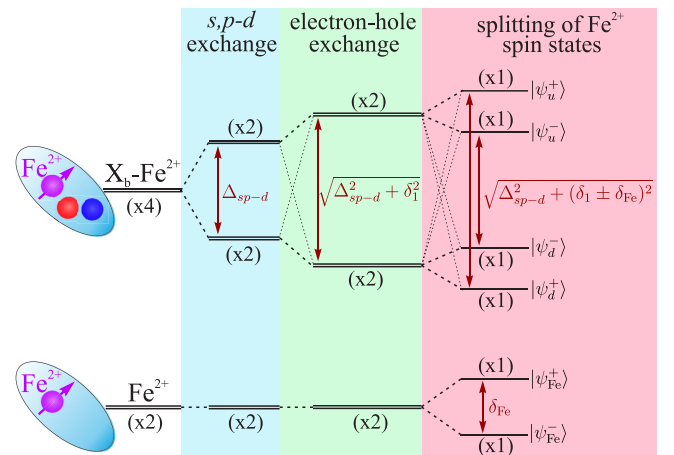


FIG. 2. The scheme illustrating the energies of both initial and final states of the bright exciton X_b recombination in a QD with a single Fe^{2+} ion (note that level spacing is not to scale). Numbers in parentheses denote the degeneracy of the energy levels. For the sake of clarity, we omitted the higher-energy states of the Fe^{2+} ion with $|S_z| < 2$ that are not populated at helium temperatures.

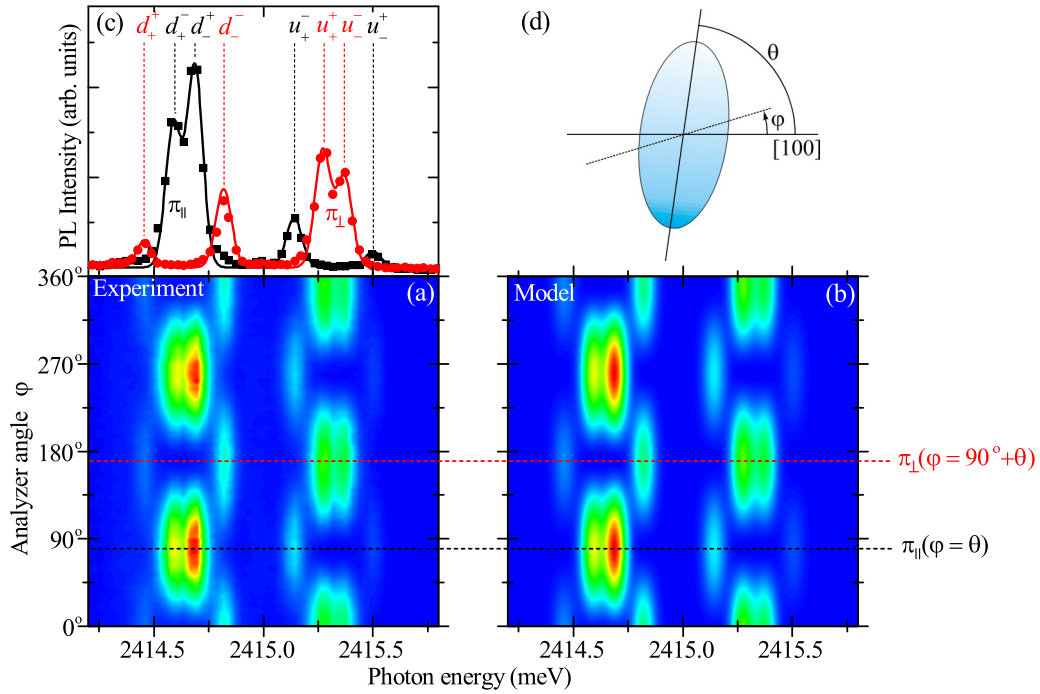


FIG. 3. (a) Color-scale map presenting the X PL spectra measured for QD2 using different orientations of detected linear polarization. The polarization angle φ is measured with respect to the $[100]$ crystallographic direction. For all spectra the continuous background was subtracted. Additionally, the subsequent spectra were corrected for a small-intensity drift of the whole QD emission as well as residual spectral diffusion (<0.03 meV) using the reference unpolarized PL signal originating from the trion recombination in the same QD. (b) Theoretical simulation of the experimental data from (a) within the frame of the spin Hamiltonian model described in the text. The exchange energies used for the fit yield $\Delta_{sp-d} = 0.53$ meV, $\delta_1 = 0.39$ meV, and $\delta_{Fe} = 0.23$ meV. (c) The X PL spectra detected in two orthogonal linear polarizations π_{\parallel} (black) and π_{\perp} [red (gray)] oriented along the principal axes $\varphi = \theta$ and $\varphi = \theta + 90^\circ$ of the electron-hole exchange interaction anisotropy (solid lines represent the model calculations). (d) Cartoon with definitions of the angles used in the discussion.

it arises due to the higher-order spin-orbit coupling and local in-plane anisotropy of the QD [20]. Regardless of its microscopic origin, such a mixing affects both initial and final configurations of the excitonic recombination. First, it splits the two Fe^{2+} spin states in the final configuration by δ_{Fe} . Second, the invoked mixing of the ion states induces also a substantial reorganization of the X_b - Fe^{2+} energy levels, leading, in general, to the presence of four nondegenerate states, as shown in Fig. 2. Thus, for an appropriately large value of δ_{Fe} , the X PL spectrum no longer consists of two emission lines but exhibits a more complex structure, as seen in the spectrum obtained for QD2 [Fig. 1(b)]. Interestingly, this spectrum still comprises two broader spectral features separated mainly by the $s, p-d$ exchange interaction, but each of these features displays also a nontrivial internal fine structure.

Insight into the general properties of the bright-X emission in a dot with a single Fe^{2+} ion is provided by our linear-polarization-resolved PL measurements of QD2. Figure 3(a) shows a series of the X PL spectra measured for different orientations φ of detected linear polarization (where $\varphi = 0^\circ$ corresponds to the $[100]$ crystallographic direction). The data clearly reveal the presence of eight distinct emission lines, which are fully linearly polarized along two orthogonal directions [the spectra detected in these two polarizations are presented in Fig. 3(c)]. This observation directly confirms that all four initial states of the X_b - Fe^{2+} system as well as the two final states of the Fe^{2+} ion are indeed nondegenerate in

the studied QD. Moreover, the optical transitions are possible between any given pair of these initial and final states. The resulting emission pattern consists of two quartets of lines separated by a pronounced central gap. For each of these quartets, the pair of stronger inner lines is orthogonally polarized to the pair of weaker outer lines. Furthermore, both the inner and outer pairs of lines within the lower-energy quartet are cross polarized to the corresponding pairs of lines from the higher-energy quartet.

IV. THEORETICAL MODEL

All observed features of the excitonic emission can be quantitatively described within the frame of a simple spin Hamiltonian model, which includes the three aforementioned interactions: the $s, p-d$ exchange, the electron-hole exchange, and the mixing of the two Fe^{2+} ion spin states with $S_z = \pm 2$. Using the basis $(|+1, +2\rangle, |-1, +2\rangle, |+1, -2\rangle, |-1, -2\rangle)$ of the exciton-ion states $|J_z, S_z\rangle$, the Hamiltonian of the X_b - Fe^{2+} system can be expressed as

$$H = \frac{1}{2} \begin{bmatrix} \Delta_{sp-d} & \delta_1 e^{-2i\theta} & \delta_{Fe} e^{-2i\beta} & 0 \\ \delta_1 e^{2i\theta} & -\Delta_{sp-d} & 0 & \delta_{Fe} e^{-2i\beta} \\ \delta_{Fe} e^{2i\beta} & 0 & -\Delta_{sp-d} & \delta_1 e^{-2i\theta} \\ 0 & \delta_{Fe} e^{2i\beta} & \delta_1 e^{2i\theta} & \Delta_{sp-d} \end{bmatrix}, \quad (1)$$

where θ and β denote the angles between the [100] crystallographic direction and the in-plane anisotropy axes of, respectively, the electron-hole exchange interaction and the mixing of the Fe^{2+} ion states. Without loss of generality, in the following analysis we will assume that $\delta_1, \delta_{\text{Fe}} \geq 0$. Analytical diagonalization of the above Hamiltonian allows us to compute four eigenstates of the $\text{X}_b\text{-Fe}^{2+}$ system. They are given by

$$|\psi_u^\pm\rangle = \cos\alpha_\pm|P^\pm\rangle + \sin\alpha_\pm|A^\pm\rangle, \quad (2)$$

$$|\psi_d^\pm\rangle = \cos\alpha_\pm|A^\pm\rangle - \sin\alpha_\pm|P^\pm\rangle, \quad (3)$$

where α_\pm stands for the mixing angles defined by

$$\tan(2\alpha_\pm) = \frac{\delta_1 \pm \delta_{\text{Fe}}}{\Delta_{sp-d}} \quad (4)$$

and

$$|P^\pm\rangle = \frac{1}{\sqrt{2}}[\pm e^{-i(\beta+\theta)}|+1,+2\rangle + e^{i(\beta+\theta)}|-1,-2\rangle], \quad (5)$$

$$|A^\pm\rangle = \frac{1}{\sqrt{2}}[\pm e^{-i(\beta-\theta)}|-1,+2\rangle + e^{i(\beta-\theta)}|+1,-2\rangle] \quad (6)$$

are the phase-rotated superpositions of the two $|J_z, S_z\rangle$ states corresponding to either the parallel or antiparallel orientation of the exciton and the ion spins. The eigenenergies of the four eigenstates of the Hamiltonian H read

$$E(|\psi_u^\pm\rangle) = \frac{1}{2}\sqrt{\Delta_{sp-d}^2 + (\delta_1 \pm \delta_{\text{Fe}})^2}, \quad (7)$$

$$E(|\psi_d^\pm\rangle) = -\frac{1}{2}\sqrt{\Delta_{sp-d}^2 + (\delta_1 \pm \delta_{\text{Fe}})^2}. \quad (8)$$

The above expressions provide valuable insight into the properties of the excitonic states in an Fe-doped QD. First, regardless of the values of the mixing terms δ_1 and δ_{Fe} , the dominant admixtures to the higher-energy (lower-energy) eigenstates $|\psi_u^\pm\rangle$ ($|\psi_d^\pm\rangle$) correspond to the basis states with parallel (antiparallel) spin alignment of the ion and the exciton. Second, since the mixing angles α_\pm depend solely on the strengths of the three considered interactions, the joint contributions of parallel (antiparallel) spin states to each of the eigenstates are independent of the in-plane anisotropy directions θ and β . In fact, the amplitude of these contributions scales with a sum or a difference of the mixing terms δ_1 and δ_{Fe} for pairs of the eigenstates with outer energies ($|\psi_u^+\rangle, |\psi_d^+\rangle$) or inner energies ($|\psi_u^-\rangle, |\psi_d^-\rangle$), respectively. This statement is also valid in regard to the values of energy splittings between the invoked pairs of the eigenstates, which are increasing functions of $|\delta_1 \pm \delta_{\text{Fe}}|$, as seen from Eq. (8) and marked in Fig. 2.

To simulate the excitonic PL spectrum, we calculate the intensities and polarizations of the optical transitions between the above-introduced eigenstates of the $\text{X}_b\text{-Fe}^{2+}$ system and the two δ_{Fe} -split eigenstates of the Fe^{2+} ion in an empty dot, which are given by

$$|\psi_{\text{Fe}}^\pm\rangle = \frac{1}{\sqrt{2}}[\pm e^{-i\beta}|+2\rangle + e^{i\beta}|-2\rangle], \quad (9)$$

with the state corresponding to the plus sign being higher energy. The PL intensity emitted in the transition $|i\rangle \rightarrow |f\rangle$

TABLE I. Relative values of square dipole moments of excitonic optical transitions in linear polarization oriented along the φ direction for a QD with a single Fe^{2+} ion [expressed using angles defined in Fig. 3(d)]. Each entry contains a value of $|\langle f|\mathcal{P}_\varphi|i\rangle|^2$ corresponding to a linearly polarized transition between a given pair, $|i\rangle$ and $|f\rangle$, of initial and final states of the excitonic recombination.

	$ \psi_{\text{Fe}}^-\rangle$	$ \psi_{\text{Fe}}^+\rangle$
$ \psi_u^+\rangle$	$\frac{1}{2}(1 - \sin 2\alpha_+) \cos^2(\varphi - \theta)$	$\frac{1}{2}(1 + \sin 2\alpha_+) \sin^2(\varphi - \theta)$
$ \psi_u^-\rangle$	$\frac{1}{2}(1 + \sin 2\alpha_-) \sin^2(\varphi - \theta)$	$\frac{1}{2}(1 - \sin 2\alpha_-) \cos^2(\varphi - \theta)$
$ \psi_d^-\rangle$	$\frac{1}{2}(1 - \sin 2\alpha_-) \sin^2(\varphi - \theta)$	$\frac{1}{2}(1 + \sin 2\alpha_-) \cos^2(\varphi - \theta)$
$ \psi_d^+\rangle$	$\frac{1}{2}(1 + \sin 2\alpha_+) \cos^2(\varphi - \theta)$	$\frac{1}{2}(1 - \sin 2\alpha_+) \sin^2(\varphi - \theta)$

with a linear polarization oriented along the φ direction is computed as a product of the initial-state occupancy and the square transition dipole moment $|\langle f|\mathcal{P}_\varphi|i\rangle|^2$, where \mathcal{P}_φ is an interband linear polarization operator. This operator can be expressed as $\mathcal{P}_\varphi = (e^{i\varphi}\mathcal{P}_+ - e^{-i\varphi}\mathcal{P}_-)/\sqrt{2}$ [35,36], where \mathcal{P}_\pm is an interband operator for σ^\pm polarized transitions that annihilate the exciton occupying $|J_z = \pm 1\rangle$ states. Using these definitions as well as the above expressions for the eigenstates, we obtain the values of $|\langle f|\mathcal{P}_\varphi|i\rangle|^2$ for the transitions between all pairs of initial and final states, which are listed in Table I. Each of these values take a general form of either $f_{\text{osc}} \cos^2(\varphi - \theta)$ or $f_{\text{osc}} \sin^2(\varphi - \theta)$, where f_{osc} denotes the corresponding (relative) oscillator strength. This result evidences that the excitonic transitions are indeed fully linearly polarized along the two orthogonal directions θ and $\theta + 90^\circ$. These directions are coincident with the principal axes of the electron-hole exchange interaction anisotropy, which demonstrates that the orientation β of the Fe^{2+} ion in-plane anisotropy has no influence on the optical spectrum.

Let us now focus on the oscillator strengths f_{osc} of the optical transitions. According to Table I, each of them has a similar form, $f_{\text{osc}} = (1 \pm \sin 2\alpha_m)/2$, where α_m stands for one of the two mixing angles α_\pm . Given that $\alpha_\pm > 0$ in the typical case of the experimentally studied QD2, we can identify the more (less) intense excitonic transitions with those exhibiting a plus (minus) sign in the expression for the oscillator strength. As such, there are two pairs of stronger transitions, $|\psi_u^\pm\rangle \rightarrow |\psi_{\text{Fe}}^\pm\rangle$ and $|\psi_d^\mp\rangle \rightarrow |\psi_{\text{Fe}}^\pm\rangle$, labeled as u_\pm^\pm and d_\pm^\mp , respectively. In agreement with the experimental data, both of these pairs are cross linearly polarized [see Fig. 3(c)]. The same polarization behavior holds also for the two pairs of weaker transitions, $|\psi_u^\mp\rangle \rightarrow |\psi_{\text{Fe}}^\pm\rangle$ and $|\psi_d^\pm\rangle \rightarrow |\psi_{\text{Fe}}^\pm\rangle$, which are labeled in Fig. 3(c) as u_\pm^\mp and d_\pm^\pm , respectively.

Notably, the fact that the excitonic PL lines originate from four different initial states hinders a direct comparison of their intensities. For example, the transitions u_\pm^+ and d_\pm^+ exhibit equal oscillator strengths; however, the PL intensity emitted in the latter transition is clearly larger in the experiment, as seen in Fig. 3(c). The major factor contributing to this effect is unequal occupancy of various initial states, which stems from a partial relaxation of the $\text{X}_b\text{-Fe}^{2+}$ system during the excitonic lifetime. In order to account for this factor, we fit the experimental

data in Fig. 3(a) with the following formula describing the excitonic PL intensity I at a given emission energy E and for the orientation φ of the detected linear polarization:

$$I(E, \varphi) = \sum_{|i\rangle, |f\rangle} \rho(|i\rangle) |\langle f | \mathcal{P}_\varphi | i \rangle|^2 g(E - E_0 - E_{|i\rangle \rightarrow |f\rangle}), \quad (10)$$

where $\rho(|i\rangle)$ is a (fitted) occupancy of the $|i\rangle$ initial state, $E_{|i\rangle \rightarrow |f\rangle}$ denotes the energy difference between the $|i\rangle$ and $|f\rangle$ states, E_0 is an overall energy shift (bare-exciton energy), and g is a Gaussian profile of the width corresponding to the resolution of our experimental setup. Such a formula perfectly reproduces our experimental results including the energies, polarization behavior, and relative intensities of all eight PL lines, as shown in Figs. 3(b) and 3(c). On this basis we determine all relevant parameters characterizing the studied QD2. As already inferred from our initial considerations, the s, p - d exchange energy $\Delta_{sp-d} = 0.53$ meV is found to dominate over the energies of the two mixing terms $\delta_1 = 0.39$ meV and $\delta_{Fe} = 0.23$ meV. Furthermore, coherent with the previous reports on II-VI QDs [34,36–39], the linear polarization orientation θ defined by the electron-hole exchange interaction anisotropy is not coincident with any particular crystallographic direction. Finally and interestingly, the occupancies $\rho(|i\rangle)$ of different initial states are found to follow closely a Boltzmann distribution with an effective temperature of about 15 K. We stress that a similar overall agreement between the experiment and the theoretical model was achieved for all studied QDs containing single Fe^{2+} ions, which confirms that our conclusions concerning the general properties of the excitonic spectrum might be regarded as representative of the studied QD system.

Having established the quantitative description of the excitonic PL spectrum in an Fe-doped QD, it is interesting to examine how the properties of this spectrum evolve upon application of an external magnetic field in the Faraday geometry. The field introduces a Zeeman splitting between different spin states of both the exciton and the ion, which gives rise to a characteristic excitonic magneto-PL spectrum. Such a spectrum measured for QD2 in the σ^- polarization of detection is shown in Fig. 4(a). The general pattern is very similar to the one previously established in Ref. [20]. It includes the presence of a distinctive crosslike feature, which is clearly visible in the range of small positive magnetic fields from $B = 0$ to about 1.5 T. The two crossing lines correspond to the excitonic transitions involving the spin flip of the Fe^{2+} ion from $S_z = \pm 2$ to $S_z = \mp 2$, which is partially allowed due to the mixing δ_{Fe} of the ion spin states. The efficiency of this mixing is naturally enhanced when the effective magnetic field acting on the ion spin vanishes. This is realized either for $B = 0$ in the absence of the exciton or for a certain positive magnetic field (1.5 T in the case of QD2), which compensates the s, p - d exchange field coming from the $|J_z = -1\rangle$ exciton emitting σ^- polarized light. On this basis one would expect the crossing lines to appear only at positive magnetic fields, as indeed observed in Ref. [20] for a relatively symmetric Fe-doped QD. However, in the case of the studied QD2, at least one out of the two crossing lines is also visible at negative fields. This is due to strong δ_1 mixing of the two X spin states $|J_z = \pm 1\rangle$

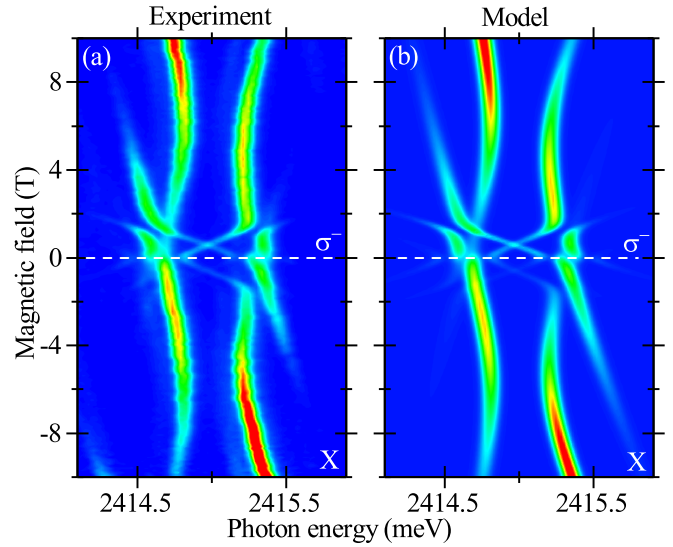


FIG. 4. (a) Color-scale map presenting the magnetic field dependence of the neutral exciton PL spectrum in QD2 (the field was applied in the Faraday geometry, i.e., along the growth axis of the sample). The data were measured in the σ^- polarization of detection. (b) Corresponding simulation of the X magneto-PL performed within the frame of the spin Hamiltonian H from Eq. (1) extended with a phenomenological diamagnetic shift term with $\gamma = 0.70$ $\mu\text{eV}/\text{T}^2$ as well as the ion and the exciton Zeeman terms with the corresponding g factors equal to $g_{Fe} = 2.2$ and $g_X = 1.7$, respectively. The values of all the other model parameters are the same as in the zero-field fit from Fig. 3(b).

that at $B > 0$ ($B < 0$) is particularly efficient for the X states associated with $S_z = -2$ ($S_z = +2$) spin projection of the Fe^{2+} ion, for which the excitonic Zeeman effect counteracts the ion-related exchange splitting. Importantly, all of the discussed details of the X magneto-PL can be described within the frame of our previously developed theoretical model based on the spin Hamiltonian H extended with an effective diamagnetic shift γB^2 term as well as two Zeeman terms, $g_{Fe}\mu_B B S_z$ and $\frac{1}{2}g_X\mu_B B J_z$, of the ion and the exciton, respectively. Using the same exchange energies determined previously from the zero-field analysis of QD2, we are able to perfectly reproduce all the features observed in the experiment, as seen in the simulation of the X magneto-PL in Fig. 4(b). The optical transitions in the presented simulation are calculated in the same manner as for the zero-field case described by Eq. (10), except that now we use the \mathcal{P}_- circular-polarization operator instead of a linear-polarization one and include the thermalization of the Zeeman-split Fe^{2+} ion spin states in the empty dot.

V. CONCLUSIONS

In conclusion, we have thoroughly characterized the fine structure of the bright-exciton PL spectrum in a CdSe/ZnSe QD with an individual Fe^{2+} ion. In particular, we have demonstrated both experimentally and theoretically that, in general, this spectrum consists of eight distinct linearly polarized emission lines, which correspond to optical transitions between all four initial states of the X_b - Fe^{2+} system and the two final states of the Fe^{2+} ion that are populated at helium

temperatures. Such a rich spectral pattern was shown to be due to δ_{Fe} mixing of the Fe^{2+} spin states and the anisotropic part δ_1 of the electron-hole exchange, which couples different spin states of X that are split by the s, p - d exchange with the magnetic ion. Based on our theoretical analysis, we conclude that a necessary condition for the presence of a maximal number of eight lines in the X PL spectrum is the coexistence of both δ_{Fe} and δ_1 mixing interactions. Otherwise, the spectral pattern is found to be much simpler, consisting of either two lines for vanishing δ_{Fe} or four lines, when $\delta_1 = 0$ but $\delta_{\text{Fe}} \neq 0$. While the former pattern is observed experimentally for some Fe-doped QDs, the latter does not seem to be realized in the case of the studied CdSe/ZnSe QD system due to relatively strong electron-hole exchange coupling. Despite such a difference in possible spectral signatures of various Fe-doped QDs, their spectra are always found to be very similar upon application of a magnetic field of a few teslas in the

Faraday geometry, which restores the pure spin symmetry of the Fe^{2+} eigenstates. This allows us to conveniently address the Fe^{2+} ion spin by optical means even in highly asymmetric QDs, which indicates that the QD anisotropy does not reduce the potential of the Fe^{2+} ion as a two-level system of presumably long spin coherence time [20].

ACKNOWLEDGMENTS

This work was supported by the Polish National Science Centre under decisions DEC-2011/02/A/ST3/00131, DEC-2015/18/E/ST3/00559, DEC-2013/09/B/ST3/02603, and DEC-2016/23/B/ST3/03437 and by the Polish Ministry of Science and Higher Education under Project No. IP2015 031674 for years 2016–2018. T.S. was supported by the Polish National Science Centre through PhD scholarship Grant No. DEC-2016/20/T/ST3/00028.

-
- [1] L. Besombes, Y. Léger, L. Maingault, D. Ferrand, H. Mariette, and J. Cibert, Probing the Spin State of a Single Magnetic Ion in an Individual Quantum Dot, *Phys. Rev. Lett.* **93**, 207403 (2004).
- [2] J. Kobak, T. Smoleński, M. Goryca, M. Papaj, K. Gietka, A. Bogucki, M. Koperski, J.-G. Rousset, J. Suffczyński, E. Janik, M. Nawrocki, A. Golnik, P. Kossacki, and W. Pacuski, Designing quantum dots for solotronics, *Nat. Commun.* **5**, 3191 (2014).
- [3] T. Smoleński, CdSe/ZnSe quantum dot with a single Mn^{2+} ion – A new system for a single spin manipulation, *J. Appl. Phys.* **117**, 112805 (2015).
- [4] B. Varghese, H. Boukari, and L. Besombes, Dynamics of a Mn spin coupled to a single hole confined in a quantum dot, *Phys. Rev. B* **90**, 115307 (2014).
- [5] M. Goryca, M. Koperski, T. Smoleński, L. Cywiński, P. Wojnar, P. Plochocka, M. Potemski, and P. Kossacki, Spin-lattice relaxation of an individual Mn^{2+} ion in a CdTe/ZnTe quantum dot, *Phys. Rev. B* **92**, 045412 (2015).
- [6] Y. Léger, L. Besombes, L. Maingault, D. Ferrand, and H. Mariette, Geometrical Effects on the Optical Properties of Quantum Dots Doped with a Single Magnetic Atom, *Phys. Rev. Lett.* **95**, 047403 (2005).
- [7] Y. Léger, L. Besombes, J. Fernández-Rossier, L. Maingault, and H. Mariette, Electrical Control of a Single Mn Atom in a Quantum Dot, *Phys. Rev. Lett.* **97**, 107401 (2006).
- [8] M. Goryca, T. Kazimierczuk, M. Nawrocki, A. Golnik, J. A. Gaj, P. Kossacki, P. Wojnar, and G. Karczewski, Optical Manipulation of a Single Mn Spin in a CdTe-Based Quantum Dot, *Phys. Rev. Lett.* **103**, 087401 (2009).
- [9] C. Le Gall, A. Brunetti, H. Boukari, and L. Besombes, Optical Stark Effect and Dressed Exciton States in a Mn-Doped CdTe Quantum Dot, *Phys. Rev. Lett.* **107**, 057401 (2011).
- [10] A. H. Trojnar, M. Korkusiński, E. S. Kadantsev, P. Hawrylak, M. Goryca, T. Kazimierczuk, P. Kossacki, P. Wojnar, and M. Potemski, Quantum Interference in Exciton-Mn Spin Interactions in a CdTe Semiconductor Quantum Dot, *Phys. Rev. Lett.* **107**, 207403 (2011).
- [11] C. Le Gall, L. Besombes, H. Boukari, R. Kolodka, J. Cibert, and H. Mariette, Optical Spin Orientation of a Single Manganese Atom in a Semiconductor Quantum Dot Using Quasiresonant Photoexcitation, *Phys. Rev. Lett.* **102**, 127402 (2009).
- [12] L. Besombes and H. Boukari, Resonant optical pumping of a Mn spin in a strain-free quantum dot, *Phys. Rev. B* **89**, 085315 (2014).
- [13] M. Goryca, M. Koperski, P. Wojnar, T. Smoleński, T. Kazimierczuk, A. Golnik, and P. Kossacki, Coherent Precession of an Individual $5/2$ Spin, *Phys. Rev. Lett.* **113**, 227202 (2014).
- [14] A. Lafuente-Sampietro, H. Boukari, and L. Besombes, Strain-induced coherent dynamics of coupled carriers and Mn spins in a quantum dot, *Phys. Rev. B* **92**, 081305 (2015).
- [15] T. Smoleński, M. Koperski, M. Goryca, P. Wojnar, P. Kossacki, and T. Kazimierczuk, Optical study of a doubly negatively charged exciton in a CdTe/ZnTe quantum dot containing a single Mn^{2+} ion, *Phys. Rev. B* **92**, 085415 (2015).
- [16] A. Kudelski, A. Lemaître, A. Miard, P. Voisin, T. C. M. Graham, R. J. Warburton, and O. Krebs, Optically Probing the Fine Structure of a Single Mn Atom in an InAs Quantum Dot, *Phys. Rev. Lett.* **99**, 247209 (2007).
- [17] O. Krebs, E. Benjamin, and A. Lemaître, Magnetic anisotropy of singly Mn-doped InAs/GaAs quantum dots, *Phys. Rev. B* **80**, 165315 (2009).
- [18] E. Baudin, E. Benjamin, A. Lemaître, and O. Krebs, Optical Pumping and a Nondestructive Readout of a Single Magnetic Impurity Spin in an InAs/GaAs Quantum Dot, *Phys. Rev. Lett.* **107**, 197402 (2011).
- [19] T. Smoleński, W. Pacuski, M. Goryca, M. Nawrocki, A. Golnik, and P. Kossacki, Optical spin orientation of an individual Mn^{2+} ion in a CdSe/ZnSe quantum dot, *Phys. Rev. B* **91**, 045306 (2015).
- [20] T. Smoleński, T. Kazimierczuk, J. Kobak, M. Goryca, A. Golnik, P. Kossacki, and W. Pacuski, Magnetic ground state of an individual Fe^{2+} ion in strained semiconductor nanostructure, *Nat. Commun.* **7**, 10484 (2016).
- [21] J. Kobak, A. Bogucki, T. Smoleński, M. Papaj, M. Koperski, M. Potemski, P. Kossacki, A. Golnik, and W. Pacuski, Direct determination of zero-field splitting for single Co^{2+} ion embedded in a CdTe/ZnTe quantum dot, [arXiv:1610.05732](https://arxiv.org/abs/1610.05732).

- [22] A. Lafuente-Sampietro, H. Utsumi, H. Boukari, S. Kuroda, and L. Besombes, Individual Cr atom in a semiconductor quantum dot: Optical addressability and spin-strain coupling, *Phys. Rev. B* **93**, 161301 (2016).
- [23] A. Lafuente-Sampietro, H. Utsumi, H. Boukari, S. Kuroda, and L. Besombes, Spin dynamics of an individual Cr atom in a semiconductor quantum dot under optical excitation, *Appl. Phys. Lett.* **109**, 053103 (2016).
- [24] A. Lafuente-Sampietro, H. Utsumi, H. Boukari, S. Kuroda, and L. Besombes, Resonant optical control of the spin of a single Cr atom in a quantum dot, *Phys. Rev. B* **95**, 035303 (2017).
- [25] J. Papierska, A. Ciechan, P. Bogusławski, M. Boshta, M. M. Gomma, E. Chikoidze, Y. Dumont, A. Drabińska, H. Przybylińska, A. Gardias, J. Szczytko, A. Twardowski, M. Tokarczyk, G. Kowalski, B. Witkowski, K. Sawicki, W. Pacuski, M. Nawrocki, and J. Suffczyński, Fe dopant in ZnO: 2+ versus 3+ valency and ion-carrier $s,p-d$ exchange interaction, *Phys. Rev. B* **94**, 224414 (2016).
- [26] J. A. Gaj and J. Kossut, Basic Consequences of $sp-d$ and $d-d$ Interactions in DMS, in *Introduction to the Physics of Diluted Magnetic Semiconductors*, edited by J. A. Gaj and J. Kossut, Springer Series in Materials Science Vol. 144 (Springer, Heidelberg, 2010), pp. 1–36.
- [27] R. Fainblat, C. J. Barrows, E. Hopmann, S. Siebeneicher, V. A. Vlaskin, D. R. Gamelin, and G. Bacher, Giant Excitonic Exchange Splittings at Zero Field in Single Colloidal CdSe Quantum Dots Doped with Individual Mn^{2+} Impurities, *Nano Lett.* **16**, 6371 (2016).
- [28] D. Gammon, E. S. Snow, B. V. Shanabrook, D. S. Katzer, and D. Park, Fine Structure Splitting in the Optical Spectra of Single GaAs Quantum Dots, *Phys. Rev. Lett.* **76**, 3005 (1996).
- [29] L. Besombes, K. Kheng, and D. Martrou, Exciton and Biexciton Fine Structure in Single Elongated Islands Grown on a Vicinal Surface, *Phys. Rev. Lett.* **85**, 425 (2000).
- [30] M. Bayer, G. Ortner, O. Stern, A. Kuther, A. A. Gorbunov, A. Forchel, P. Hawrylak, S. Fafard, K. Hinzer, T. L. Reinecke, S. N. Walck, J. P. Reithmaier, F. Klopff, and F. Schäfer, Fine structure of neutral and charged excitons in self-assembled In(Ga)As/(Al)GaAs quantum dots, *Phys. Rev. B* **65**, 195315 (2002).
- [31] J. Puls, M. Rabe, H.-J. Wünsche, and F. Henneberger, Magneto-optical study of the exciton fine structure in self-assembled CdSe quantum dots, *Phys. Rev. B* **60**, R16303 (1999).
- [32] V. D. Kulakovskii, G. Bacher, R. Weigand, T. Kümmell, A. Forchel, E. Borovitskaya, K. Leonardi, and D. Hommel, Fine Structure of Biexciton Emission in Symmetric and Asymmetric CdSe/ZnSe Single Quantum Dots, *Phys. Rev. Lett.* **82**, 1780 (1999).
- [33] B. Patton, W. Langbein, and U. Woggon, Trion, biexciton, and exciton dynamics in single self-assembled CdSe quantum dots, *Phys. Rev. B* **68**, 125316 (2003).
- [34] J. Kobak, T. Smoleński, M. Goryca, J.-G. Rousset, W. Pacuski, A. Bogucki, K. Oreszczuk, P. Kossacki, M. Nawrocki, A. Golnik, J. Plachta, P. Wojnar, C. Kruse, D. Hommel, M. Potemski, and T. Kazimierczuk, Comparison of magneto-optical properties of various excitonic complexes in CdTe and CdSe self-assembled quantum dots, *J. Phys. Condens. Matter* **28**, 265302 (2016).
- [35] A. V. Koudinov, I. A. Akimov, Y. G. Kusrayev, and F. Henneberger, Optical and magnetic anisotropies of the hole states in Stranski-Krastanov quantum dots, *Phys. Rev. B* **70**, 241305 (2004).
- [36] T. Kazimierczuk, T. Smoleński, M. Goryca, L. Kłopotowski, P. Wojnar, K. Fronc, A. Golnik, M. Nawrocki, J. A. Gaj, and P. Kossacki, Magnetophotoluminescence study of intershell exchange interaction in CdTe/ZnTe quantum dots, *Phys. Rev. B* **84**, 165319 (2011).
- [37] Y. Léger, L. Besombes, L. Maingault, and H. Mariette, Valence-band mixing in neutral, charged, and Mn-doped self-assembled quantum dots, *Phys. Rev. B* **76**, 045331 (2007).
- [38] T. Kazimierczuk, T. Smoleński, J. Kobak, M. Goryca, W. Pacuski, A. Golnik, K. Fronc, L. Kłopotowski, P. Wojnar, and P. Kossacki, Optical study of electron-electron exchange interaction in CdTe/ZnTe quantum dots, *Phys. Rev. B* **87**, 195302 (2013).
- [39] T. Smoleński, T. Kazimierczuk, M. Goryca, P. Wojnar, and P. Kossacki, Fine structure of a resonantly excited p -shell exciton in a CdTe quantum dot, *Phys. Rev. B* **93**, 195311 (2016).